

Temperature-controlled CO, CO₂ and NO_x sensing in a diesel engine exhaust stream

Osvaldo L. Figueroa^a, Chonghoon Lee^a, Sheikh A. Akbar^b, Nicholas F. Szabo^a, Joseph A. Trimboli^a, Prabir K. Dutta^c, Naoto Sawaki^d, Ahmed A. Soliman^e, Henk Verweij^{b,*}

^a The Ohio State University (OSU), Center for Industrial Sensors and Measurements (CISM), 2041 College Road, 291A Watts Hall, Columbus, OH 43210-178, USA

^b The Ohio State University (OSU), Department of Materials Science and Engineering, 291A Watts Hall, 2041 College Road, Columbus, OH 43210-1178, USA

^c The Ohio State University (OSU), Department of Chemistry, 120W 18th Avenue, Columbus, OH 43210-1302, USA

^d NGK Spark Plugs (USA) Inc., Automotive Group, 46929 Magellan Drive, Wixom, MI 48393-3699, USA

^e The Ohio State University (OSU), Center for Automotive Research, 930 Kinnear Road, Columbus, OH 43212-1433, USA

Received 1 July 2004; received in revised form 30 November 2004; accepted 9 December 2004

Available online 21 January 2005

Abstract

Results are presented for in situ measurement of CO₂, NO_x and CO concentrations in exhaust emitted from an automotive diesel engine. These data were obtained with a series of temperature-controlled sensor probes and compared to exhaust concentrations measured simultaneously with an exhaust motor analyzer. The CO₂ sensor is a Nernstian type with a Li₂CO₃|Au sensing electrode, a Li₃PO₄ electrolyte and a Li₂TiO₃ + TiO₂|Au reference electrode. The total NO_x sensor measures the difference between potential responses of two porous Pt electrodes on an ion-conducting stabilized cubic zirconia support. The potential difference results because one Pt electrode is covered with a catalyst to achieve a locally equilibrated NO_x mixture, whereas the other electrode exposed to the sensing gas mixture, pre-equilibrated at a different temperature. The CO sensor is a resistive type and responds to selective sorption of reducing species. All sensor types have simple planar configurations but require accurate temperature control to deal with significant fluctuations in the engine exhaust stream. A constant sensor temperature of typically 400 °C is achieved with a ceramic heater strip and tight control using a direct digital PID algorithm. The NO_x sensor requires a second temperature-controlled pre-conditioning filter. This filter is integrated in the probe and controlled with a thermo-coax heating wire and another PID implementation. Generally, the sensors responses in the engine agree with the laboratory tests, but calibration errors resulted due to lack of thermal homogeneity of the sensor. In addition, some drift is observed due to particulate contamination from the exhaust stream. The CO₂ sensor appeared to be the most robust, though the probe signal may have been influenced by the evacuation effect at high gas velocities present in the car exhaust.

© 2004 Elsevier B.V. All rights reserved.

Keywords: High temperature sensors; Zeolite-based sensors; Automotive exhaust sensors; Potentiometric sensors; Resistive sensors

1. Introduction

In view of the increasingly strict laws for emissions from motor vehicles and other sources of pollutants, the need for a new generation of in situ, cost effective and reliable gas sensors has become a high priority [1]. Such sensors must be

able to provide a stable and unambiguous signal in harsh environments as exist in: (i) the convective pass after the burner section of a coal-fired power plant and (ii) the exhaust of a compression-ignition direct-injection (CIDI, diesel) engine. These sensors can potentially be used in feedback control of systems operation or as an indicator that preventive maintenance is needed [2]. Sensors-based on solid-electrolyte and semiconducting ceramics, operating at typically 400 °C or higher are good candidates for such applications. Gas species

* Corresponding author. Tel.: +1 614 2476987; fax: +1 614 6884949.

E-mail address: verweij.1@osu.edu (H. Verweij).

of interest are NO_x, CO, hydrocarbons (HC), and to some extent O₂, CO₂ and H₂O. Previous work in CISM has resulted in several high temperature sensing concepts for these gases [3–16] that are briefly discussed here.

1.1. CO₂ sensor

The CO₂ sensor is of the Nernstian type with a multilayer structure, consisting of a Li₂CO₃ sensing electrode (top), a Li₃PO₄ solid-electrolyte (middle), and a reference electrode made of Li₂TiO₃ + TiO₂ (bottom) [15,16]. The lithium phosphorous oxide solid electrolyte-based sensor shows good selectivity, sensitivity and a linear response that follows the Nernst equation:

$$\Delta\Phi_{\text{cell}} = \frac{\mu_{\text{Li}_2\text{CO}_3}^0 + \mu_{\text{TiO}_2}^0 - \mu_{\text{Li}_2\text{TiO}_3}^0 - \mu_{\text{CO}_2}^0}{2F} - \frac{RT}{2F} \ln \frac{p_{\text{CO}_2}}{p^0} \quad (1)$$

where $\Delta\Phi_{\text{cell}}$ is the cell voltage (sensor signal), F the Faraday constant, R the gas constant, T the absolute temperature, p_{CO_2} the gas-sensing pressure, and p^0 the standard pressure, 101,325 Pa. $\mu_{\text{Li}_2\text{CO}_3}^0$, $\mu_{\text{TiO}_2}^0$, $\mu_{\text{Li}_2\text{TiO}_3}^0$, and $\mu_{\text{CO}_2}^0$ are the standard state chemical potentials. The sensor requires a background p_{O_2} of the order of 10 kPa and a working temperature between 400 and 500 °C.

1.2. Total NO_x sensor

The total NO_x sensor is a mixed potential type, where the sensing electrode consists of a thin porous Pt film while the reference electrode consists of a similar porous Pt film but covered with a Pt-loaded zeolite Y¹ catalyst [7]. The role of the catalyst is to provide local equilibration at the reference electrode between NO and NO₂ at the sensor operating temperature and p_{O_2} background of the order of 10 kPa. NO and NO₂ do not easily equilibrate at the sensing electrode without the presence of a catalyst so that a mixed potential response is measured between the sensing and the reference electrodes. For NO₂ in excess of NO, the mixed potential can be expressed as [7]:

$$\Delta\Phi_{\text{m}} = \frac{RT}{F} \ln \left(\frac{k_{\text{NO}_2}[\text{NO}_2]}{k_{\text{O}_2}[\text{O}_2] + k_{\text{NO}}[\text{NO}]} \right) \quad (2)$$

where k 's are the electrochemical reaction rate constants.

This sensor concept can be used to obtain a 'total NO_x' signal by pre-equilibrating the gas mixture (NO and NO₂) at different temperature with the same type of (Pt-loaded zeolite) catalyst. Pure NO and NO₂ shows a sensor response that is proportional to their partial pressure but in mutually opposite directions. The absolute values of the proportionality constants are different, and the pre-equilibration temperature is chosen such that the NO–NO₂ mixture at the sensing

electrode produces a significant signal. The pre-equilibration temperature treatment has the additional advantage of removal, by oxidation, of interference from other gases such as CO and hydrocarbons. The oxidation products CO₂ and H₂O do not affect sensor operation. The sensor can be used between 400 and 700 °C. Below 400 °C, the ionic conductivity of zirconia electrolyte becomes too low and above 700 °C zeolite decomposes.

1.3. CO sensor

The CO sensor is of the semiconductor type. A thick film is made of anatase TiO₂ particles mixed with 8 wt.% CuO and 10 wt.% La₂O₃, and an organic solvent. The additives are for catalytic oxidation of interfering hydrocarbons [8,9]. The mixture is applied on an alumina support, heat-treated, and provided with two Au electrodes to measure the resistance. First, oxygen from the ambient adsorbs on the exposed surface of the grains, and extracting electrons from the material, forms chemisorbed oxygen species. This leads to the formation of a depletion region and the electrical conductivity is determined by the height of the Schottky barrier (qV_s) between the TiO₂ grains.

$$\sigma = \sigma_0 \exp \left(\frac{-qV_s}{RT} \right) \quad (3)$$

When exposed to a reducing gas such as CO, the adsorbed CO reacts with the adsorbed oxygen species, releasing the trapped electron back to the conduction band, subsequently lowering the barrier height and increasing the conductivity. Although these thick film sensors are inexpensive, they are prone to interference from other co-existing gases such as hydrocarbons and H₂O.

1.4. Sensor design and control

Under ideal laboratory circumstances, the above-mentioned sensors have a repeatability, reproducibility and stability of O₂ (10%). They are promising because of their potential cost-effectiveness and robustness in high temperature environments such as utility boilers and automotive exhaust applications. To use them in such environments a number of conditions need to be met:

- Eqs. (1)–(3) show significant T -dependence of the sensing signal. This implies that in a fluctuating exhaust environment the sensing temperature must be controlled to a constant value, typically within 1 °C.
- The NO_x sensor as proposed requires a pre-equilibration of the gas mixture at a temperature, significantly different from the sensing temperature.
- The sensing materials should, to some extent, be shielded from direct contact with turbulent gases (flames) and particulate contamination.

These requirements can be met by attaching the sensor on top of a temperature-controlled heating strip. This heating

¹ Faujasite, official International Zeolite Association code: FAU.

strip, in turn, must be surrounded by a protective filter that allows for sufficiently fast gas diffusion but, at the same time, optimum thermal homogeneity at the sensor, and protects it from the main stream fluctuations and particulate contamination.

The filter can also be used for pre-equilibration by combining it with a heating element. Controlling the temperature of the filter has the additional advantage of more stable temperature control of the sensor because it decouples the sensor further from the fluctuating environment. To avoid the need of active cooling elements, the sensor and filter operating temperatures must be chosen higher than the average maximum temperature of the gas stream. For prototype sensor packages, sufficiently stable temperature control is obtained by employing an ideal PID algorithm:

$$\text{output} = \frac{100}{x_P} \left(\Delta T + \int_0^t \frac{\Delta T}{t_I} dt + t_D \frac{d\Delta T}{dt} \right) \quad (4)$$

in which output is the set point for the heating element power controller, x_P the proportional band, ΔT the set-point – actual T , t the elapsed process time, t_I the integration time constant, and t_D the derivative action time constant. Relevant temperatures can be derived from heating element resistances or carefully positioned thermocouples or resistors. Optimum settings for x_P , t_I and t_D result in tight control (close and fast set-point conformity) after startup or in response to process changes or perturbations. Such settings are related to process gain and time characteristics of the control configuration, and these depend on the detailed sensor construction, gas composition, pressure, and flow, power controller characteristics and scaling. For separate heaters, an initial estimate for optimum settings can be obtained with the Zeigler–Nichols method [17]. Those estimates can be used as a starting set for a trial and error optimization for simultaneous control of both sensor and filter temperatures. The sensor and filter control loops can be strongly interacting and no tailor-made optimization approach exists for that case as yet. Experimental sets of optimum control parameters, obtained for a number of well-chosen conditions, may be used to derive an (adaptive) optimum control parameter function. This function depends on one or more temperatures and gas conditions. Future scenarios foresee development of more dedicated algorithms, or that control parameters are obtained directly from in situ analysis or artificial intelligence treatment of control loop gain, dynamics, and gas sensor data (auto-tuning). Advances in microprocessor technology have made that, complex control software can be implemented at a cost-price that is small compared to the costs of sensor packaging and wiring.

1.5. Approach and scope

The objective of this paper is to present and discuss the results obtained with a temperature-controlled sensor package for monitoring of CO_2 , NO_x , and CO present in automotive diesel engine exhaust. The study presented here was carried

out in collaboration with industrial partners to demonstrate feasibility without trying to optimize detailed packaging and controller designs. Initial studies were carried out with the CO_2 sensor because that was the most robust, followed by the NO_x sensor, requiring a temperature-controlled pre-filter, and finally the CO sensor, being the most vulnerable to contamination. The sensors were applied on a heater strip supplied by NGK Spark Plugs, Inc. The sensor probe was made to fit the standard 18 mm \times 1.5 mm thread, and the filter heating element was made with Thermocoax heating wire. Temperatures were derived from thermocouples near the sensor and from heating wire resistances. All control and measurement electronics was interfaced with a PC; data acquisition and control software was implemented on a LabView 6.1 platform. Single loop PID control was implemented for both heater systems and with constant parameter settings, optimized for a set of typical conditions.

2. Experimental

All heat treatments of sensor materials took place in air with a heating rate of 6 °C/min and natural cooling after soak unless indicated otherwise.²

2.1. CO_2 sensor preparation

A 6 mm \varnothing and 1 mm thick electrolyte pellet is prepared, starting from a mixture of Li_3PO_4 with 5 mol% SiO_2 ³ as a sintering aid. About 0.4 g of mixed powder is cold pressed, single-sided and uniaxially in a hardened 8 mm \varnothing stainless steel die⁴ using a pressure of 6.9 MPa. The pellet is sintered in air for 6 h at 800 °C on a flat alumina ceramic plate at a heating and cooling rate of 2 °C/min. Two separate Au ink contacts are hand painted⁵ on top of the pellet and a 250 μm \varnothing Au wire is bonded to the contacts using the same gold ink. The Au ink is cured by heating for 1 h at 700 °C with a 5 °C/min heating/cooling rate. After curing the contacts, a Li_2CO_3 sensing electrode, and a $\text{Li}_2\text{TiO}_3 + \text{TiO}_2$ reference electrode are hand painted on top of the Au contacts. The paints are made by mixing relevant powders⁶ with α -terpineol solvent. The Li_2CO_3 electrode is heat-treated for 1 h at 600 °C. The $\text{Li}_2\text{TiO}_3 + \text{TiO}_2$ is then heat-treated for 1 h at 700 °C.

2.2. NO_x sensor preparation

The NO_x sensors are prepared on 0.5 mm thick, 5 mm \times 5 mm single crystalline Ytria-Stabilized Zirconia

² Description of experimental details in this paper is necessarily brief. More details can be obtained by contacting the corresponding author.

³ Both 99.5% grade, Alpha Aesar, Ward Hill, MA, USA.

⁴ Mode C, Wabash, IN, USA.

⁵ C5789, Heraeus, Hanau, Germany.

⁶ 99% grade Li_2CO_3 , and 99.9% grade TiO_2 : Alpha Aesar, Ward Hill, MA, USA. Li_2TiO_3 : Lithium Corp. of America, Bessemer City, NC, USA.

(YSZ) substrates.⁷ About 50 μm thick Pt ink⁸ electrodes are hand painted on the substrate. About 127 μm \varnothing Pt wires are bonded to the electrodes by pressing them in a drop of Pt ink on top of the electrodes. The sensor is then placed in the furnace and cured for 2 h at 1250 °C. Zeolite powder⁹ was loaded with Pt as described in [18], and mixed with α -terpineol solvent to form a paste. The paste is painted over one of the electrodes and then heated for 1 h at 500 °C.

2.3. CO sensor preparation

Two 250 μm \varnothing Au wires are tied into holes machined in a 0.5 mm thick, 8 mm \times 8 mm alumina substrate with interdigitated gold electrodes, screen printed on its surface. Au paste is then painted on the base of the wire, and the alumina surrounding the wire hole, to bond the wire to the electrodes. The sensor is prepared starting by milling anatase titania¹⁰ in isopropanol for 4 h using zirconia balls.¹¹ The solvent is removed by natural evaporation, followed by heating the resultant powder at 6 °C/min to 800 °C with a 6 h soak. The resulting powder is mixed with 30 wt.% organic binder,¹² 30 wt.% solvent,¹³ 0.15 ml dispersant¹⁴ to make a thick paste. The paste is then hand-painted on the alumina substrate, followed by heating for 2 h at 200 °C to remove the organic binders and heating for 6 h at 800 °C to form the sensor.

2.4. Temperature-controlled sensors

Fig. 1 is a schematic drawing of the temperature-controlled sensor with an active, temperature-controlled pre-filter. Fig. 2 shows a picture of one of the probes used in car exhaust experiments. The stainless steel sensor housing is made in the OSU workshop and provided with a 18 mm \times 1.5 mm thread, as used for automobile oxygen sensors. Holes in the nose of the assembly provided a gas diffusion port as well as protection from the main stream and particulate contamination. Any remaining empty space after mounting the sensor heating assembly and the pre-filter is filled with quartz wool, to stabilize the entire construction. All wiring is drawn through a modified connector that is secured to the package, providing strain relief to the wires. A layer of a sealing compound¹⁵ is applied at the back of the sensor. The sensor heater is made of a 2 mm thick 4 mm \times 50 mm alumina multi-layer strip with a screen printed heating element embedded at one end of the strip and heating a \sim 4 mm \times 4 mm¹⁶ area up to 600 °C.

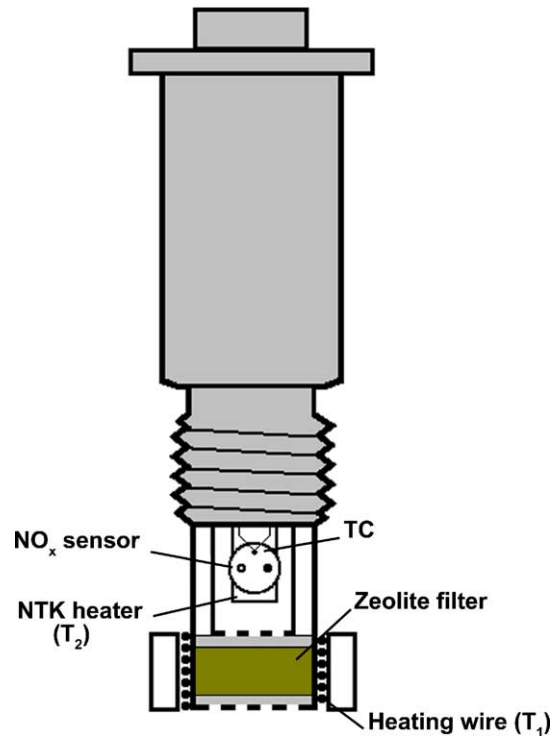


Fig. 1. Sensor package for the NO_x sensor.



Fig. 2. Connector and sensor probe without pre-filter heater.

The heater strip is centered inside a 9.53 mm outer diameter (OD), 6.35 mm inner diameter (ID), 25.4 mm long Mullite tube.¹⁷ A 3.18 mm OD, 0.51 mm ID, 25.4 mm long Mullite four-bore tube,¹⁸ guiding the signal and 0.25 mm \varnothing K-type¹⁹

⁷ MTI Corp., Richmond, CA, USA.

⁸ A4731, Engelhard-CLAL LP, Carteret, NJ, USA.

⁹ LZ-52, Union Carbide, Houston, TX, USA.

¹⁰ 99.9%+, Sigma-Aldrich Corp., St. Louis, MO, USA.

¹¹ 8005A, Fisher Scientific, Hampton, NH, USA.

¹² V-801, Heraeus, Hanau, Germany.

¹³ 5V-507, Heraeus, Hanau, Germany.

¹⁴ DISPERSBYK-110, BYK Chemie, Wesel, Germany.

¹⁵ Resbond 907GF, Cotronics Corp., Brooklyn, NY, USA.

¹⁶ NGK Spark Plugs (USA) Inc., Automotive Group, Wixom, MI, USA.

¹⁷ Part # 66636, CoorsTek, Golden, CO, USA.

¹⁸ Part # 66676, CoorsTek, Golden, CO, USA.

¹⁹ Part #: CHAL-010, Omega Engineering Inc., Stamford, CT, USA.

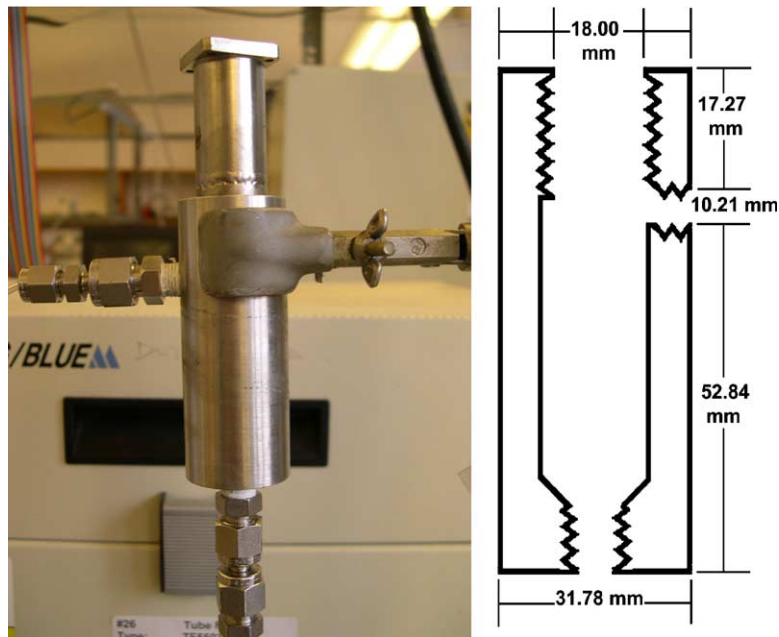


Fig. 3. Laboratory test chamber.

thermocouple wires, is placed on top of the heater inside the 9.53 mm OD Mullite tube. Any remaining empty space in that tube is filled with cement²⁰ to stabilize the heater + four-bore tube position. The sensor assembly (CO₂, CO and NO_x) is bonded to the heater surface with a ceramic adhesive.²¹ The thermocouple hot junction is positioned near the sensing surface. The 9.53 mm OD Mullite tube is centered in the stainless steel housing with a cone fitting and a 9.53 mm ferrule²² fixed to the tube with a ceramic adhesive.²³

The catalytic pre-filter for the NO_x sensor is made by packing Pt-loaded zeolite powder between two porous sintered vitreous silica disks in the filter ‘nose’ of the housing. To heat the filter up to 600 °C, a coaxial heating wire²⁴ is coiled inside a 19.05 mm ID alumina tube²⁵ around the package nose (see also Fig. 1).

Temperature measurements were taken by 0.25 mm Ø K-type thermocouples²⁶ located: (i) close to the sensor location, (ii) between the zeolite filter heater coil and the ‘nose’ and (iii) at the entrance of the exhaust, 127 mm from the sensor location.

A stable performance in the fluctuating car exhaust environment of these thermocouples was obtained by securing their position with a ceramic cement.

²⁰ Omegabond 300, Omega Engineering Inc., Stamford, CT, USA.

²¹ 904 Zirconia, Cotronics Corp., Brooklyn, NY, USA.

²² Swagelok Cleveland, USA.

²³ Ceramabond 569, Aremco Products Inc., Valley Cottage, NY, USA.

²⁴ Type ZE Ac15/15-29/TI/CB 15/KZ 0506/2m, Thermocoax, Suresnes, France.

²⁵ Part # 66455, CoorsTek, Golden, CO, USA.

²⁶ Part #: CHAL-010, Omega Engineering Inc., Stamford, CT, USA.

2.5. Laboratory testing of sensors

To test the sensors in the laboratory, we use a stainless steel chamber as shown in Fig. 3. This chamber has 18 mm × 1.5 mm threading to hold the sensor.

2.5.1. Gas mixing instrument

A gas mixing instrument composed of mass flow controllers is used to produce a volumetric mixture of gases. The instrument is composed of four 100 sccm (standard cubic centimeters per minute) SEC-4400M²⁷ mass flow controllers (MFCs) with nitrogen calibration, two 100 sccm SEC-4400M MFCs with oxygen calibration, and one 3 sccm SEC-7320M MFC with nitrogen calibration. To be able to control two of the MFCs with the computer, power to these units is provided by a Sierra instruments 900 series power supply.²⁸ Power and control to the other MFCs is provided by five PAC-5S power supplies and readouts. The actual gas flow rate is calibrated with a digital flow meter.²⁹

Concentrations of gas species are indicated as [species]. The O₂ source is compressed air; low [CO₂]s are achieved with 1% CO₂ in N₂; high [CO₂]s with pure CO₂; [NO]s with 600 ppm NO in N₂; [NO₂]s with 2000 ppm NO₂ in N₂; [CO]s with 2000 ppm CO in N₂. Adjustment of overall gas concentration is done with a pure N₂ cylinder. All gases are obtained from cylinders.³⁰

²⁷ STEC Inc., Kyoto, Japan.

²⁸ Sierra Instruments Inc., Monterey, CA, USA.

²⁹ Model 520, Fisher Scientific, Hampton, NH, USA.

³⁰ Praxair Inc., 39 Old Ridgebury Road, Danbury, CT 06810, USA.

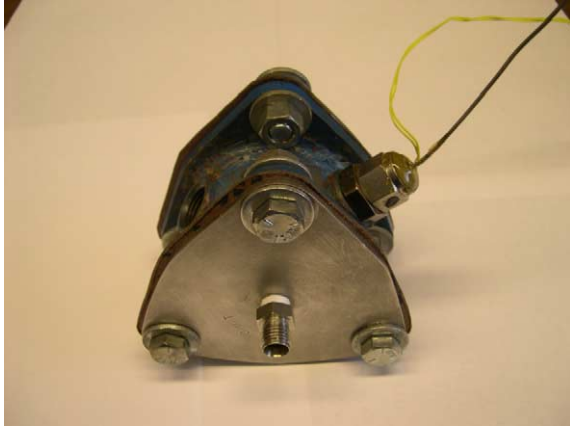


Fig. 4. Fitting used for tests with a controlled filter temperature, mounted on a T-outlet right after the engine. Besides the sensor probe at right, a connection lead feed-through for the thermocoax heater and the thermocouple (yellow) are shown.

2.6. Engine testing of sensors

For the automotive exhaust analysis a 2.4L, 5 cylinder, 1997 Fiat diesel engine is used. The engine speed and torque are controlled by a dynamometer interfaced with a PC. Accurate engine exhaust data is acquired with an analyzer³¹ capable of measuring [CO], [CO₂], [NO_x], [O₂] and total hydrocarbons (THC). For CO₂ and CO sensor testing, the sensor probe is mounted in an oxygen sensor port along the exhaust pipe of the diesel engine. For NO_x sensor testing the probe with the filter heater is mounted in a steel chamber. The tests with the pre-heated filter are carried out in a special fitting, shown in Fig. 4. The sample port of the analyzer is at a distance of about 127 mm from the sensor location.

2.7. Measurement and control instrumentation

2.7.1. Hardware

External digital communication is achieved primarily with an IEEE-488 cable bus. The PC is connected to this bus with a USB-IEEE-488 adapter.³² Power to the sensor strip heater and pre-filter thermocoax wire is provided with DC power supplies³³ with an IEEE-488 interface. A high input impedance digital multimeter³⁴ with an IEEE-488 interface is used to acquire the sensor signals. An SCXI modular system³⁵ is used for data acquisition and temperature control, with the following components:

- An SCXI-1000 four module chassis that provides power to data acquisition modules, and handles signal routing

between the SCXI system and a PCI-MIO-16E-4 12 bits multipurpose input–output (MIO) data acquisition card, installed in the PC. The output channels of the latter are used for control of two of the MFCs.

- An SCXI-1102C 32 channel analog input signal conditioning module for high-accuracy measurement of thermovoltages, analog Fiat engine parameter and Horiba analyzer signals. The Horiba provides accurate [CO] (high), [CO] (low), [CO₂], [NO_x], [THC], and [O₂]. All signals are measured in differential mode to diminish the risk of electrical noise.
- An SCXI-1303 isothermal connection block used with the SCXI-1102C to provide accurate thermocouple cold-junction compensation, and a thermocouple ground connection.

A user interface, measurement control and data acquisition program is realized on a LabVIEW 6.1 platform for SCXI, power supplies, and multimeter interfacing and temperature control with built-in direct digital PID controllers.

3. Results and discussion

3.1. CO₂ sensor

3.1.1. Laboratory tests

To test the CO₂ sensor, a volumetric gas mixture ranging from 500 ppm to 50% CO₂ in a background of 10% O₂ was led through the test chamber, shown in Fig. 3, at a total flow rate of 210 sccm. The sensor was heated at 10 °C/min to the target temperature of 350 °C in 10% O₂ and balance N₂. The measured [CO₂] was nearly identical to that obtained in regular furnace tests. After diesel engine operation we tested the sensor again in the test chamber and observed some drift at higher [CO₂]. When we removed the sensor from the package, we noticed some exhaust particle contamination on the sensors surface. We also noticed that some of the electrode material deposited on the surface came loose, caused by engine vibrations.

3.1.2. Engine testing

Testing was done without the pre-filter present. Roughly the same torque versus time program was applied every day for 4 subsequent days. Fig. 5 shows the exhaust temperature to vary between 100 and 350 °C. The sensor temperature controller was tuned with one fixed set of PID parameters that was sufficiently relaxed to maintain stable control for all torque settings. Fig. 6 shows that temperature was stable within ±1 °C between torque changes. The largest temperature fluctuation at torque transients was 3 °C. The sensor strip heater resistance is shown in Fig. 7 and found to decrease with increasing torque (with the sensor surface controlled to a constant temperature). This decrease corresponds to more heat supplied to the surface from the exhaust. The actual effective sensor temperature is likely to be between the measured

³¹ Motor exhaust analyzer MEXA-7500DEGR, Horiba Instruments Inc., Ann Arbor, MI, USA.

³² Type USB-A, National Instruments Corp., Austin, TX, USA.

³³ Type E3642A, Agilent Technologies, Palo Alto, CA, USA.

³⁴ Type 34401A, Agilent Technologies, Palo Alto, CA 95303, USA.

³⁵ National Instruments Corp., Austin, TX, USA.

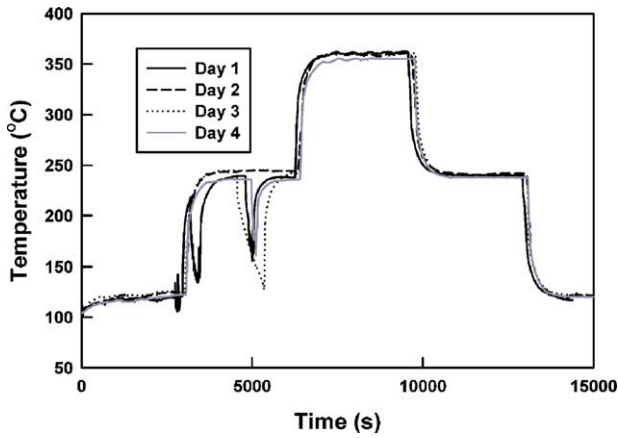


Fig. 5. Exhaust gas temperature.

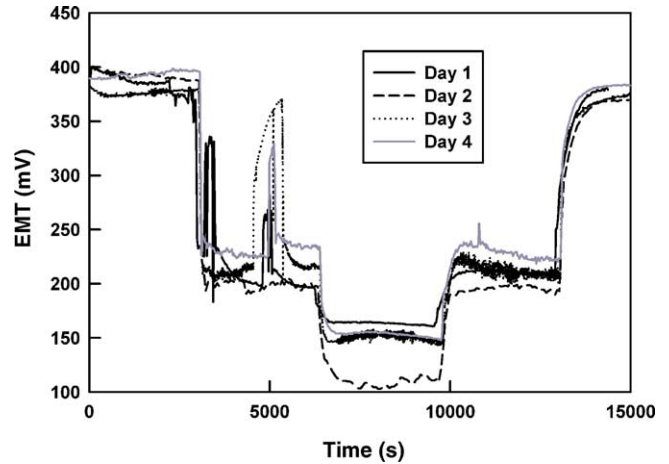


Fig. 8. Sensor EMF.

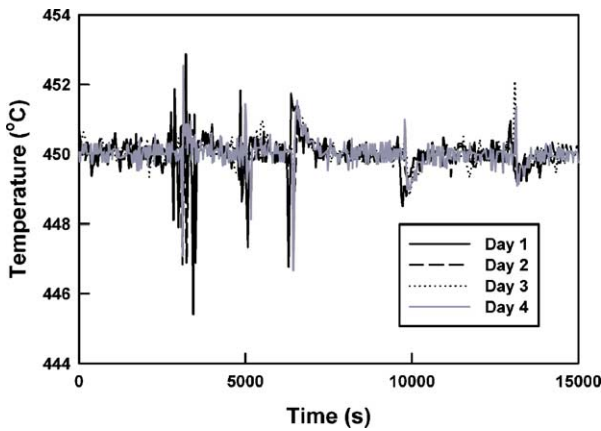


Fig. 6. Sensor temperature.

surface and heater temperatures so that small systematic corrections to the derived $[CO_2]$ may be necessary.

Fig. 8 shows the Nernstian CO_2 sensor response, and Fig. 9 the actual $[CO_2]$ during the 4 days of testing. The fact that the sensor signals during 1 day testing showed a nearly perfect correlation with the actual concentration is very encouraging.

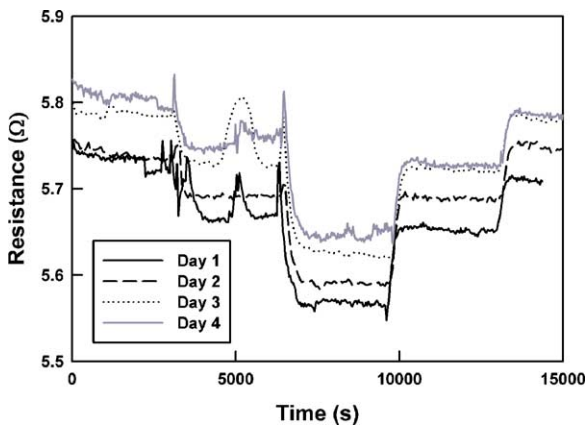


Fig. 7. Heater resistance.

The sensor signals at similar $[CO_2]$, obtained on subsequent days showed small but significant differences in response, in particular for the highest $[CO_2]$ during the second day. This might be explained by the particulate contamination of the sensors, observed after testing.

Slight variations in $[NO_x]$ were observed during testing that did not seem to influence the sensor response. $[THC]$ remained nearly constant except for a sudden temporary but significant change during day 2 that did not influence the CO_2 sensor response. No significant variations in $[CO]$ and $[O_2]$ were observed during testing.

Fig. 10 shows calibration curves generated with sensor response data, obtained with the lab test setup and during engine testing. As seen, the two tests show a significant difference. This same effect was also found in a preliminary experiment and is not yet fully explained. One important aspect is that during engine testing the gas flow rate is orders of magnitude higher than the few hundred sccm used during the laboratory tests. These high engine velocities may evacuate the sensor probe chamber while keeping the relative mixture composition constant. This would result in a lower $[CO_2]$ than what is effectively measured by the motor exhaust analyzer. In addition, the significantly different thermal environments during

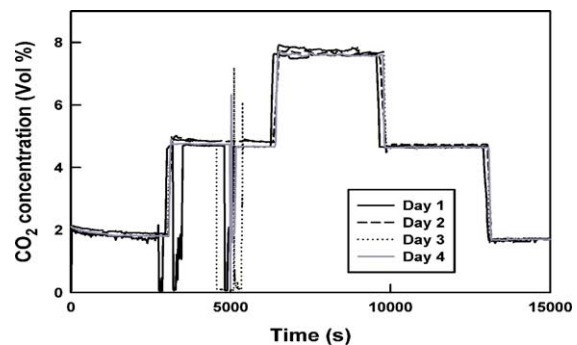


Fig. 9. Motor exhaust analyzer $[CO_2]$.

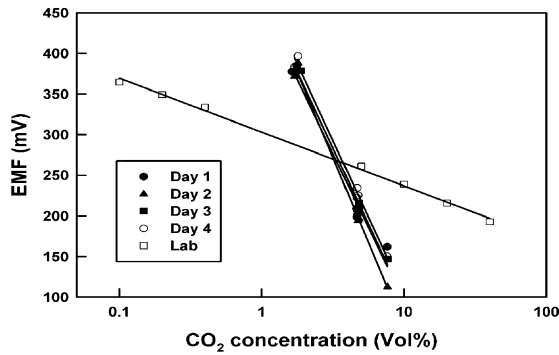


Fig. 10. Calibration curves for the CO₂ sensor, obtained in the laboratory test setup and during engine testing (bundle of 4 lines).

lab and engine tests may have influenced the signal. Both effects can be addressed with a better design. Nonetheless, the sensor CO₂ response could be used for a local total pressure measurement by comparison with [CO₂] measured by the analyzer.

3.2. NO_x sensing

3.2.1. Laboratory testing

To test the NO_x sensor, 100–400 ppm NO or NO₂ in a background of 3% O₂ was led through the test chamber at a flow rate of 200 sccm. The sensor was slowly heated to the set point in a mixture of 3% O₂ and balance N₂. The sensor and heater temperature were varied between 300 and 500 °C to obtain an equal response to NO and NO₂.

Fig. 11 shows the NO_x sensor response to a sequence of [NO] = 200 and 400 ppm, and [NO₂] = 200 and 400 ppm at optimum sensor heater and pre-filter temperature settings of 450 and 400 °C, respectively.

Besides equilibrating NO and NO₂, the second function of the zeolite filter is to oxidize CO to CO₂, to avoid CO interference. This resulted in virtually no influence of CO additions on the NO_x signals.

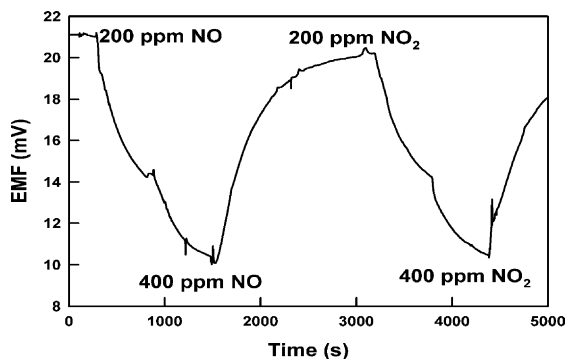


Fig. 11. NO_x sensor response to a sequence of two [NO] and two [NO₂]s at optimum settings of the sensor and pre-filter temperature of 450 and 400 °C, respectively.

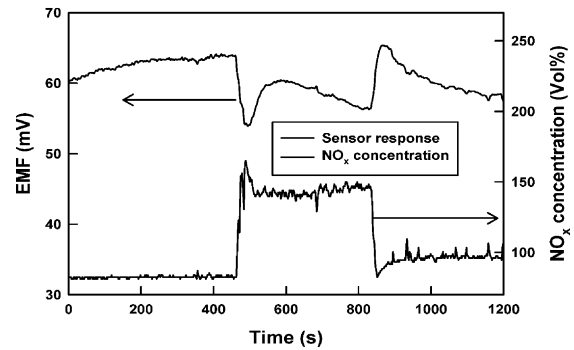


Fig. 12. NO_x sensor response vs. motor exhaust analyzer reading (right hand scale).

3.2.2. Engine testing

During an initial test we were able to keep both the sensor heater and the zeolite filter temperature within 0.5 °C and observed significant but unsteady responses to NO_x changes. In a second test, for which we present results here, we were unable to tune the pre-filter heater but observed its temperature to be in the appropriate range. Sensor heater fluctuations during torque changes were within 2.5 °C.

Fig. 12 shows the sensors response to a change in [NO_x]. The sensor responded as fast as the analyzer but showed some drift at a constant [NO_x] ascribed to internal thermal equilibration.

[CO], [THC], and [O₂] remained fairly constant at one torque setting and changed step-wise upon transients, but without the peaks in the NO_x signals. The fact that the NO_x sensor responded to those peaks gave additional confidence that interference by other gases was virtually absent. However, the quality of the NO_x sensor response did not yet justify a quantitative comparison with the motor exhaust analyzer results.

3.3. CO sensing

3.3.1. Laboratory testing

To test the CO sensor, 200–1000 ppm CO in a background of 5% O₂ was led through the test chamber at a flow rate of 100 sccm. During the test, the sensor temperature was kept within ±0.2 °C. The sensor signal showed a good correlation with step-wise changes in [CO], but showed some drift after returning to earlier [CO] values. The drift can be ascribed to a developing thermal homogenization of the sensor. No sensitivity to NO_x, CO₂ or CH₄ was observed while interference by O₂, H₂O and larger hydrocarbons can be expected.

After engine tests we observed roughly the same response though more noisy. When we opened the sensor probe we noticed that the surface of the sensor was covered with some particulate matter.

3.3.2. Engine testing

Testing was done without the pre-filter present. The sensor temperature was kept constant within ±5 °C for most of the

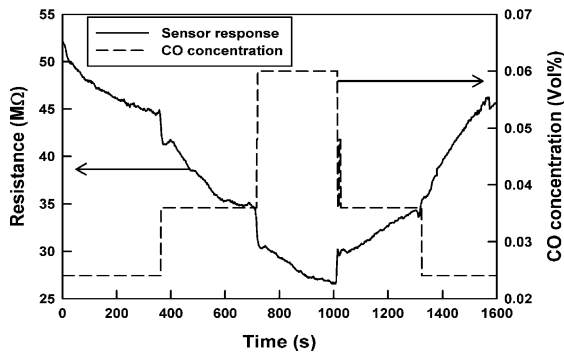


Fig. 13. CISM CO sensor vs. motor exhaust analyzer CO reading (right hand scale).

test with 20 °C fluctuations upon torque transition, followed by stabilization within 1 °C. Temperature control was lost at a torque of 217 N m when the exhaust temperature became higher than the sensor set-point of 400 °C. Fig. 13 shows the sensors response to changes in [CO]. The sensor response correlated with that of the analyser, but never reached a steady value for the duration of the test.

4. Conclusions

The results demonstrate that meaningful signals can be obtained for [CO₂], [NO_x], and [CO] in a CIDI engine exhaust stream using temperature-controlled simple planar ceramic sensors. Stable temperature control was realized with a PID-controlled heater strip. The NO_x sensor required pre-conditioning with a temperature-controlled catalytic filter. Since both the sensor and the pre-filter are in thermal contact, controller tuning in various environments can be tedious and is a subject for further study. Pre-conditioning of the analyte gas temperature is thought to be beneficial for any gas-sensing application because it better decouples the local sensor temperature from the exhaust temperature. Controller tuning in a commercially viable concept can be done with model-based algorithms or artificial intelligence methods.

Both CO₂ and CO sensing suffered from particulate contamination that can be addressed by application of a pre-filter as in the NO_x sensor, but without catalytic activity. In addition sensor calibration was found to be affected by not yet optimized thermal design of the sensor. The CO₂ sensor appeared to be the most robust and allowed for quantitative comparisons with laboratory calibrations. Those comparisons indicated that evacuation of the sensor probe chamber at high gas velocities in the exhaust may lead to additional calibration effects. On the other hand, this can also be exploited to obtain the absolute total gas pressure and gas velocities from [CO₂]. This will enable better temperature control and more accurate [NO_x] and [CO] measurements in a sensor array inside an optimized probe design. Future designs should include improved thermal design of the probe, better protection from

particulate contamination and improved mechanical integrity of the sensors and thermocouples and their connections.

Acknowledgements

This work was supported by the National Science Foundation contract number EEC-9523358, the Department of Energy contract number DE-FC26-03NT41615, and NASA-GMI contract no. NNC04AA48A.

References

- [1] N.F. Szabo, C.H. Lee, J.A. Trimboli, O.L. Figueroa, R. Ramamoorthy, H. Verweij, P.K. Dutta, S.W. Midlam-Mohler, A.A. Soliman, S.A. Akbar, Ceramic-based chemical sensors, probes and field-tests in automotive engines, *J. Mater. Sci.* 38 (2003) 4239–4245.
- [2] A.A. Soliman, P.K. Dutta, O.L. Figueroa, J. Jackson, A NO_x sensor for diesel emission control, in: *Proceedings of the International Conference on Engines for Automobile, Capri-Naples, 2003*.
- [3] L.D. Birkefeld, A.M. Azad, S.A. Akbar, Carbon monoxide and hydrogen detection by anatase modification of titanium dioxide, *J. Am. Ceram. Soc.* 75 (1992) 2964–2968.
- [4] P.K. Dutta, A. Ginwalla, B. Hogg, B. Patton, B. Chwieroth, Z. Liang, P. Gouma, M. Mills, S.A. Akbar, Interaction of carbon monoxide with anatase surfaces at high temperatures: optimization of a carbon monoxide sensor, *J. Phys. Chem. B* 103 (1999) 4412–4422.
- [5] N. Savage, S.A. Akbar, P.K. Dutta, Titanium dioxide-based high temperature carbon monoxide selective sensor, *Sens. Actuators B* 72 (2001) 239–248.
- [6] N. Savage, B. Chwieroth, A. Ginwalla, B.R. Patton, S.A. Akbar, P.K. Dutta, Composite n-p semiconducting titanium oxides as gas sensors, *Sens. Actuators B* 79 (2001) 17–27.
- [7] N.F. Szabo, P.K. Dutta, Strategies for total NO_x measurement with minimal CO interference utilizing a microporous zeolitic catalytic filter, *Sens. Actuators B* 88 (2003) 168–177.
- [8] N. Savage, S.A. Akbar, P.K. Dutta, Titanium dioxide-based high temperature carbon monoxide selective sensor, *Sens. Actuators B* 72 (2001) 239–248.
- [9] P.I. Gouma, S. Banerjee, M.J. Mills, TiO₂-based gas sensors as thick or thin films: an evaluation of the microstructure, *Ceram. Trans.* 100 (1999) 419–428.
- [10] Y. Chiang, C.C. Wang, S.A. Akbar, Calcium zirconate for the monitoring of hydrocarbons, *Sens. Actuators B* 46 (1998) 208–212.
- [11] A. Kohli, C.C. Wang, S.A. Akbar, Niobium pentoxide as a lean-range oxygen sensor, *Sens. Actuators B* 56 (1999) 121–128.
- [12] A.K.M.S. Chowdhury, S.A. Akbar, S. Kapileshwar, J.R. Schorr, A rugged oxygen gas sensor with solid reference for high temperature applications, *J. Electrochem. Soc.* 148 (2001) G91–G94.
- [13] B. Narayanan, S.A. Akbar, P.K. Dutta, A phosphate-based proton conducting solid electrolyte hydrocarbon gas sensor, *Sens. Actuators B* 87 (2002) 480–486.
- [14] C. Reddy, P.K. Dutta, S.A. Akbar, Detection of CO in a reducing, hydrous environment using CuBr as electrolyte, *Sens. Actuators B* 92 (2003) 351–355.
- [15] C. Lee, S.A. Akbar, C.O. Park, Potentiometric CO₂ gas sensor with lithium phosphorous oxynitride electrolyte, *Sens. Actuators B* 80 (2001) 234–242.
- [16] C.O. Park, C. Lee, S.A. Akbar, J. Hwang, The origin of oxygen dependence in a potentiometric CO₂ sensor with Li-ion conducting electrolytes, *Sens. Actuators B* 88 (2003) 53–59.

- [17] J.G. Ziegler, N.B. Nichols, Optimum settings for automatic controllers, *Trans. ASME* 64 (1942) 759–768.
- [18] Y. Hasegawa, K. Kusakabe, S. Morooka, Selective oxidation of carbon monoxide in hydrogen-rich mixtures by permeation through a platinum-loaded Y-type zeolite membrane, *J. Membr. Sci.* 190 (2001) 1–8.

Biographies

Oswaldo L. Figueroa received his M.Sc. degree in materials science and engineering from The Ohio State University in 2003. His interests include sensors, instrumentation and control.

Chonghoon Lee received his Ph.D. degree in 2004 in the Department of Materials Science and Engineering from The Ohio State University. He is currently involved in development of sensor arrays for fire detection and thin film-based electrochemical CO₂ gas sensors.

Sheikh A. Akbar is a Professor of materials science and engineering and Founder of the NSF Center for Industrial Sensors and Measurements (CISM) at Ohio State University. He obtained his Ph.D. degree from Purdue University in 1985. His current research focuses on microstructure–property relations of electroceramics (chemical sensors and fuel cell electrodes) both in bulk and thin-film forms.

Nicholas F. Szabo received his Ph.D degree in chemistry in 2003 from The Ohio State University. He is currently employed with Conductive Technologies, Pennsylvania.

Joseph A. Trimboli is a graduate student in CISM at the present time.

Prabir K. Dutta received his Ph.D. degree in chemistry in 1978 from Princeton University. After 4 years of industrial research at Exxon Research and Engineering Company, he joined The Ohio State University, where currently he is the Robert K. Fox Professor and Chairman of the Department of Chemistry. His research interests are in the area of microporous materials, including their synthesis, structural analysis and as hosts for chemical and photochemical reactions.

Naoto Sawaki received his Ph.D. degree in engineering management in 2004 from the Kennedy-Western University. He is currently the manager of the Technical Center and Advanced Products Group of the NGK Spark Plugs (USA) Inc. Current activities include, gas sensors, control modules, and glow plugs.

Ahmed A. Soliman received his Ph.D. degree in 1997 from The Ohio State University. He is currently the Industrial Director of the Center for Automotive Research and Intelligent Transportation (CAR-IT) at OSU. Current activities include on- and off-board engine and vehicle diagnostics; powertrain control; engine modeling; and the development of gas sensors for hostile environment.

Henk Verweij received his Ph.D. degree in chemical engineering in 1980 from Eindhoven Technical University, The Netherlands. He was scientific coworker at Philips Research Labs for 17 years, full professor at the University of Twente for 9 years and since 2001 Orton Chair in Ceramic Engineering in the Department of materials science of OSU. His interests include colloidal and thermal processing of ceramics, related control and instrumentation and application of ceramic membranes. He is currently the director of CISM.